Development 133, 263-273 doi:10.1242/dev.02195

The conserved oligomeric Golgi complex acts in organ morphogenesis via glycosylation of an ADAM protease in *C. elegans*

Yukihiko Kubota[1], Mitsue Sano[1], Saori Goda[2], Norio Suzuki[1] and Kiyoji Nishiwaki[1,*]

In *C. elegans*, the gonad acquires two U-shaped arms through directed migration of gonadal distal tip cells (DTCs). A member of the ADAM (a disintegrin and metalloprotease) family, MIG-17, is secreted from muscle cells and localizes to the gonadal basement membrane where it functions in DTC migration. Mutations in *cogc-3* and *cogc-1* cause misdirected DTC migration similar to that seen in *mig-17* mutants. Here, we report that COGC-3 and COGC-1 proteins are homologous to mammalian COG-3/Sec34 and COG-1/ldlBp, respectively, two of the eight components of the conserved oligomeric Golgi (COG) complex required for Golgi function. Knockdown of any of the other six components by RNA interference also produces DTC migration defects, suggesting that the eight components function in a common pathway. COGC-3 and COGC-1 are required for the glycosylation and gonadal localization of MIG-17, but not for secretion of MIG-17 from muscle cells. Furthermore, COGC-3 requires MIG-17 activity for its action in DTC migration. Our findings demonstrate that COG complex-dependent glycosylation of an ADAM protease plays a crucial role in determining organ shape.

KEY WORDS: ADAM protease, *C. elegans*, COG complex, Glycosylation, Organogenesis

INTRODUCTION

Secreted proteins are required to guide the migration of gonadal distal tip cells (DTCs) and shape the gonad in *C. elegans* (Kimble and Hirsh, 1979; Hedgecock et al., 1987). One of the best-characterized guidance molecules is UNC-6/netrin, which is secreted from neurons on the ventral midline and is required for dorsally oriented DTC migration (Hedgecock et al., 1990; Ishii et al., 1992; Serafini et al., 1996; Wadsworth et al., 1996). Gonad shape and DTC directional migration are also regulated by two different secreted ADAM family proteases, GON-1 and MIG-17 (Blelloch and Kimble, 1999; Blelloch et al., 1999; Nishiwaki et al., 2000). GON-1 is required for both DTC motility and the expansion of gonadal arms. MIG-17 is required for the control of the direction of DTC migration, but not motility per se, and is secreted from body wall muscle cells and accumulates in the gonadal basement membrane. Remodeling of basement membranes by these ADAM proteases appears to be requisite for DTC migration and gonad morphogenesis.

The DTCs in *mig-29* and *mig-30* mutants show misdirected migration similar to that seen in *mig-17* mutants. We have molecularly cloned *mig-29* and *mig-30* and found that they encode homologs of COG-3/Sec34 and COG-1/ldlBp, respectively, which are components of the conserved oligomeric Golgi (COG) complex – a multisubunit protein complex associated with the periphery of the Golgi in mammalian cells (Ungar et al., 2002). Therefore, *mig-29* and *mig-30* were renamed *cogc-3* and *cogc-1*, respectively, where *cogc* stands for COG component. The COG complex, also called the ldlCp complex, Sec34/Sec35p complex and GTC complex, has been identified independently by several groups working in both yeast and mammalian systems. The COG complex functions in multiple aspects of intracellular vesicle trafficking, including that between the endoplasmic reticulum (ER) and Golgi, between Golgi cisternae and from endosomes to Golgi (Krieger et al., 1981; Wuestehube et al., 1996; Walter et al., 1998; Spelbrink and Nothwehr, 1999; Whyte and Munro, 2001; Suvorova et al., 2002). Biochemical and electron microscopic analyses of the mammalian COG complex have identified eight protein components: COG-1-4 form lobe A of the complex, whereas COG-5-8 form lobe B (Ungar et al., 2002; Loh and Hong, 2004). Genetic experiments in *S. cerevisiae* have implicated each of these components in vesicular transport from the ER to Golgi. Disruption of any one of the lobe A components causes severe growth defects in yeast, whereas disruption of lobe B components results in only mild growth defects (Whyte and Munro, 2001; Ram et al., 2002). Genetic analysis in mutant Chinese hamster ovary (CHO) cells showed that COG-1/ldlBp and COG-2/ldlCp are required for proper glycosylation of low-density lipoprotein receptor (LDLR) (Kingsley et al., 1986). The *Drosophila* gene, *four way stop*, encodes a homolog of COG-5 that is essential for spermatocyte cytokinesis, elongation of spermatids and maintenance of Golgi morphology in males (Farkas et al., 2003). Recently, COG-7 was shown to be a member of a novel class of proteins involved in human congenital disorder of glycosylation (CDG), which causes multisystemic developmental abnormalities, often leading to death. In individuals with CDG who have a COG-7 defect, protein glycosylation and glycosyltransferase trafficking are affected because of the destabilization of the COG complex (Wu et al., 2004). These genetic and biochemical analyses suggest that the components of the COG complex are functionally distinct and have important cellular functions; however, the roles that these components play in organogenesis remain largely unexplored.

We now report that the *C. elegans* COG complex is crucial for organ morphogenesis. The *C. elegans* genome encodes homologs for all eight components of the mammalian COG complex. We found that two of the *C. elegans* lobe A components, COGC-3 and COGC-1, are required for proper glycosylation and gonadal

[1]RIKEN Center for Developmental Biology, Chuo-ku, Kobe 650-0047, Japan.
[2]PRESTO, Japan Science and Technology Corporation, Kawaguchi, Saitama 332-0012, Japan.

*Author for correspondence (e-mail: nishiwak@cdb.riken.jp)

Accepted 1 November 2005

localization of the MIG-17 protease, which controls gonadal DTC migration. In addition, we show that the intracellular localization and expression of a membrane-bound Golgi enzyme, nucleoside diphosphatase (NDPase), MIG-23, is abnormal in *cogc-3* and *cogc-1* mutants. We have previously shown that MIG-23 is required to achieve proper glycosylation of MIG-17 in muscle cells (Nishiwaki et al., 2004). These results suggest that the COG complex acts in gonad morphogenesis by regulating Golgi enzymes such as MIG-23, thereby affecting the glycosylation and function of the MIG-17 ADAM protease.

MATERIALS AND METHODS

Strains and culture conditions

Worms were grown at 20°C (Brenner, 1974). The following mutations were used: *cogc-3(k181)*, *cogc-1(k179)* (this work), *unc-11(e47*, *n2954)* (Brenner, 1974; Nonet et al., 1999), *lin-17(rh95*, *n3090)* (Sawa et al., 1996), *unc-119(e2498)* (Maduro and Pilgrim, 1995) and *mig-17(k174)* (Nishiwaki et al., 2000).

Genetic mapping

Genetic mapping experiments assigned both *cogc-3(k181)* and *cogc-1(k179)* mutations between *lin-17* and *unc-11* on linkage group *I*. The *cogc-3* and *cogc-1* genes were cloned by SNP mapping (Wicks et al., 2001) followed by transposon tagging. *Tc4* was inserted between nucleotide positions 8913/8914 of the genomic clone, Y71F9AM in *cogc-3*. *Tc1* was inserted between nucleotide positions 80618/80619 of Y54E10A in *cogc-1*.

Microscopy

Nomarski and fluorescence microscopy were performed using a Zeiss Axioplan 2 microscope. To score the gonadal DTC migration defects, the trajectories of DTCs were deduced from the final shape of the gonad arms. The localization of MIG-23-GFP, YFP-TRAM, mRFP-SP12 and COGC-3 in body wall muscle cells was analyzed using a confocal laser scanning microscope (Radiance 2100 Rainbow, BioRad) equipped with a C-apochromat 63× (water immersion; NA 1.2) lens and controlled by Lasersharp 2000 software (BioRad).

DNA constructs

The following primers were used to amplify the *cogc-3* genomic fragment: 5′-GATGCCGTCAAGAACAAGGAGAAGAGATCG-3′ and 5′-TTCT-TGTTGGAATGTGGGAAAAGGAAGCAG-3′. The following primers were used to amplify the *cogc-1* genomic fragment: 5′-GGCACGG-ACAAGTCGTCGCGTTGAAATATG-3′ and 5′-CTGCAAGGCTACCT-ATGCCTGCCTTGTGTTGG-3′. *mec-7p::mig-17::GFP*, *unc-54p::mig-23::GFP* and *mig-17::GFP* were constructed previously (Nishiwaki et al., 2000; Nishiwaki et al., 2004). *mig-17::Venus* was constructed by replacing the coding region of GFP in the *mig-17::GFP* plasmid with that of the *Venus* gene (encoding a yellow fluorescent protein variant) (Nagai et al., 2002). The *myo-2p::YFP::TRAM* plasmid was kindly provided by Tom A. Rapoport (Rolls et al., 2002). The *unc-54p::mRFP* fusion gene was constructed by joining the fragments containing the *unc-54* promoter region with *mRFP*, a coding region for monomeric red fluorescent protein, kindly provided by Roger Y. Tsien (Campbell et al., 2002). The *unc-54p::mRFP::SP12 gene* was constructed by inserting the *unc-54p::mRFP* fragment to the *Not*I site of plasmid SP12, which was kindly provided by Anne Spang (Poteyaev et al., 2004). *arIs37[*p*myo-3::ssGFP] I* was used to analyze endocytosis and secretion (Fares and Greenwald, 2001a; Fares and Greenwald, 2001b). *mec-7p::cogc-3 and unc-54p::cogc-3* were constructed by joining the fragments containing the *unc-54* or *mec-7* promoter regions with the *cogc-3* cDNA fragment and a 1.8 kb *cogc-3* terminator fragment amplified by PCR. A full-length *cogc-3* cDNA, yk863b10, was used.

Production of transgenic animals

DNA mixtures were first injected into *unc-119(e2498)* animals (Mello et al., 1991), and the transgenic arrays were transferred to *cogc-3(k181);unc-119(e2498)* or *cogc-1(k179);unc-119(e2498)* animals by mating. The genomic *cogc-3* PCR fragment was injected at 30 μg/ml with 50 μg/ml of the marker plasmid *sur-5::GFP*, 10 μg/ml of *unc-119*$^+$ plasmid pDP#MM016B (Maduro and Pilgrim, 1995) and 60 μg/ml pBR322. The genomic *cogc-1* PCR fragment was injected at 10 μg/ml with 80 μg/ml *sur-5::GFP*, 10 μg/ml *unc-119*$^+$ plasmid and 40 μg/ml pBR322. *unc-54p::cogc-3* was injected at 20 μg/ml with 70 μg/ml *sur-5::GFP,* 10 μg/ml *unc-119*$^+$ plasmid and 50 μg/ml pBR322. *mig-17::GFP* was injected at 20 μg/ml with 10 μg/ml *unc-119*$^+$ plasmid and 120 μg/ml pBR322. *mig-17::Venus* was injected at 20 μg/ml with 10 μg/ml *unc-119*$^+$ plasmid and 120 μg/ml pBSII KS(–). To construct animals for touch cell expression experiments, *mec-7p::mig-17::GFP* was injected at 100 μg/ml with 10 μg/ml *unc-119*$^+$ plasmid and 40 μg/ml pBR322. *mec-7p::cogc-3* was injected at 20 μg/ml with 10 μg/ml *unc-119*$^+$ plasmid and 120 μg/ml pBR322. To construct animals carrying both *mec-7p::mig-17::GFP* and *mec-7p::cogc-3,* 100 μg/ml *mec-7p::mig-17::GFP* and 20 μg/ml *mec-7p::cogc-3* were co-injected with 10 μg/ml *unc-119*$^+$ plasmid and 20 μg/ml pBR322. *unc-54p::mig-23::GFP* was injected at 10 μg/ml with 10 μg/ml *unc-119*$^+$ plasmid and 130 μg/ml pBSIIKS(–). *unc-54p::mRFP::SP12* was injected at 50 μg/ml with 70 μg/ml *unc-54p::mig-23::GFP*, 10 μg/ml *unc-119*$^+$ plasmid and 20 μg/ml pBSIIKS(–). *myo-2p::YFP::TRAM* was injected at 5 μg/ml with 10 μg/ml *unc-119*$^+$ plasmid and 135 μg/ml pBSIIKS(–).

Identification of *C. elegans* COG components and L1 soaking RNAi

The amino acid identities between the COG components of *C. elegans* and human are 23% (COGC-1), 26% (COGC-2), 30% (COGC-3), 33% (COGC-4), 22% (COGC-5), 23% (COGC-6), 19 % (COGC-7) and 20% (COGC-8) using the program GENETYX (Software Development). The expected protein from *W01B6.9* (*cogc-7*) has relatively weak overall homology with human COG-7 (Fig. 2C), although the similarity is greater in the coiled-coil region; by contrast, it shows no significant similarity to yeast Cog7p. RNAi experiments were carried out as described (Maeda et al., 2001).

Preparation of antisera

The N-terminal residues 34-260 of COGC-3 tagged with GST were produced in *Escherichia coli*. A synthetic peptide (EKEMEGKRESLR-EMVGRR) corresponding to a region of the COGC-1 N terminus was coupled to keyhole limpet hemocyanin to use for an antigen. Rabbit antiserum against COGC-3 was affinity purified on columns fixed with histidine-tagged COGC-3 polypeptide. The rabbit antiserum against the COGC-1 peptide was also affinity purified using the synthetic peptide.

Western blot analysis

Worms were disrupted by glass beads in a buffer containing 50 mM Tris-HCl (pH 7.4), 200 mM NaCl, protease inhibitor cocktail (Roche) and 1% (v/v) Triton X-100. The samples were immunoblotted with rabbit anti-GFP IgG (1:1000, Molecular Probes), mouse anti-α-tubulin IgG 12G10 (1:1000, J. Frankel and M. Nelson, Developmental Studies Hybridoma Bank, University of Iowa), anti-COGC-3 (1 μg/ml), anti-COGC-1 (1 μg/ml) or anti-MIG-23 (Nishiwaki et al., 2004) (1:1000) at room temperature for 1 hour followed by incubation with peroxidase-conjugated anti-rabbit IgG or anti-mouse IgG (1:5000, Amersham Pharmacia Biotech) at room temperature for 1 hour.

Immunoprecipitation and PNGase F treatment

The worm lysates were incubated with rabbit anti-GFP (1:1000, Molecular Probes) or anti-COGC-3 (1 μg/ml) at 4°C for 3 hours. Samples were precipitated with protein A-Sepharose beads (Amersham Biosciences). Normal rabbit IgG (Genzyme TECHNE) was used as a control antibody. PNGase F treatment (New England BioLabs) was performed according to the manufacturer's instructions.

In situ staining

For whole-mount immunohistochemistry, samples were processed as described by Yamaguchi et al. (Yamaguchi et al., 1983), except that they were immersed in methanol at –20°C for 5 minutes followed by acetone at –20°C for 5 minutes. After blocking in 2% bovine serum albumin (BSA) in phosphate-buffered saline (PBS), samples were incubated with anti-COGC-3 (1 μg/ml) or mouse monoclonal anti-GFP IgG (3E6, 1:1000; Molecular Probes) in PBS containing 1% BSA at 4°C for 12 hours. Samples were then incubated with secondary antibodies TRITC donkey anti-rabbit IgG (Jackson), Texas Red donkey anti-rabbit IgG

(Jackson) or fluorescein donkey anti-mouse IgG (Jackson) diluted 1:200 in PBS containing 1% BSA at room temperature for 1 hour and with DAPI (2 μg/ml; Wako) at room temperature for 10 minutes. For frozen sections, animals were fixed with 4% paraformaldehyde in PBS for 12 hours on ice. After washing in PBS, they were resuspended sequentially in 10, 20 and 30% sucrose in PBS at 4°C. After the animals sank to the bottom of the Tissue-Tek Cryomold (Miles), the overlying sucrose solution was removed and OCT compound (Miles) was added. Frozen sections (10 μm) were prepared using a cryostat (MICROM). After blocking the sections with 2% BSA in PBS, samples were incubated with rabbit anti-COGC-3 (1 μg/ml) or rabbit anti-GFP (1:1000, Molecular Probes) in PBS containing 1% BSA for 12 hours at 4°C, with TRITC donkey anti-rabbit IgG (1:100; Jackson) in PBS containing 1% BSA for 1 hour, with fluorescein phalloidin (10 U/ml; Molecular Probes) for 1 hour, or with DAPI (2 μg/ml; Wako) for 10 minutes at room temperature.

RESULTS

cogc-3 and *cogc-1* mutations affect DTC migration

The *C. elegans* hermaphrodite gonad is bi-lobed, one lobe each in the anterior-right and posterior-left areas of the body cavity (Fig. 1A). Wild-type animals have U-shaped gonadal arms (Fig. 1B), in contrast to the variously abnormal shapes of the arms in *mig-17* mutants resulting from meandering DTC migration (Fig. 1C). To

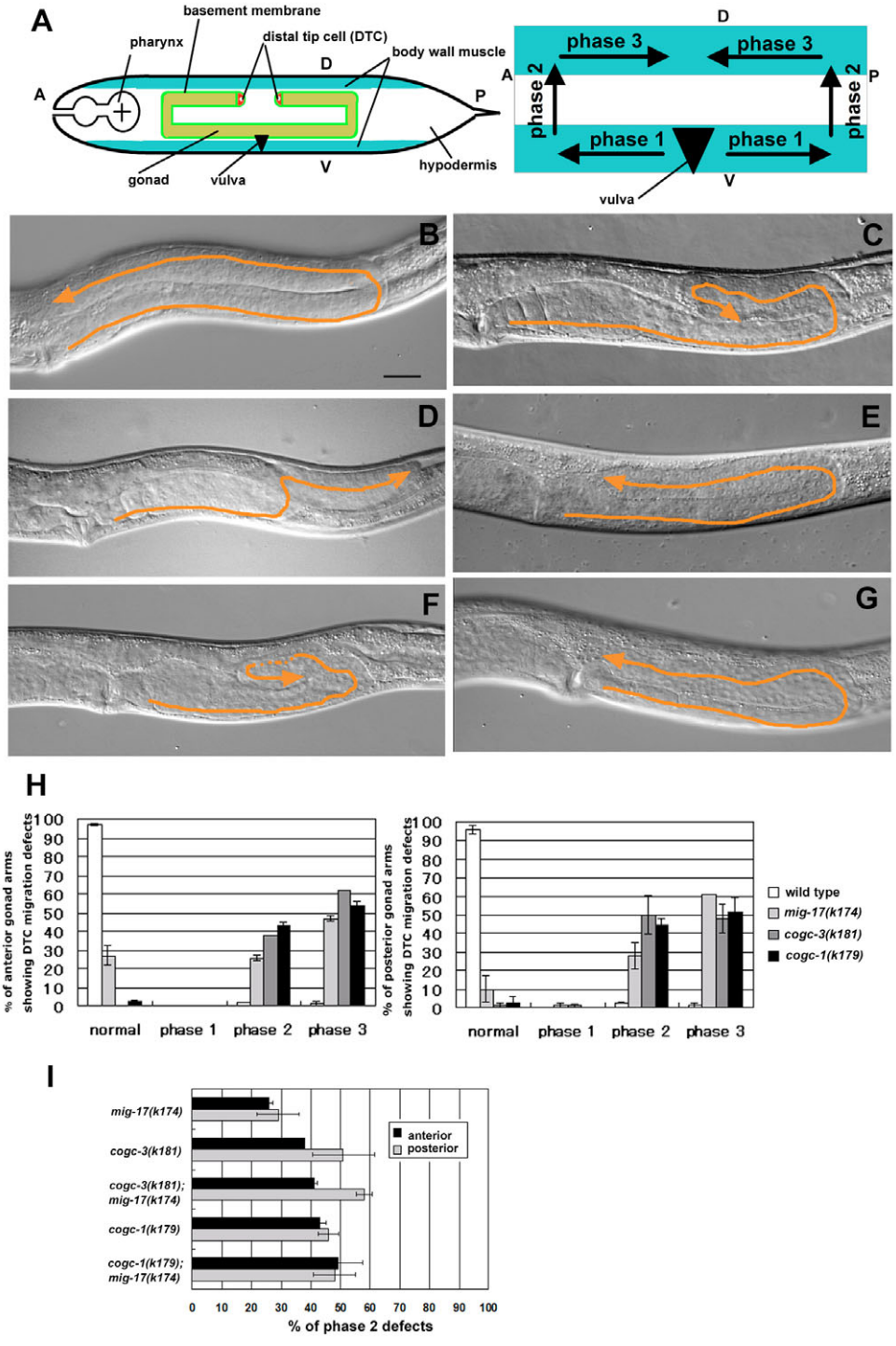

Fig. 1. Wild-type and mutant gonad morphology. (**A**) Schematic diagrams of gonad morphology in the wild-type hermaphrodite (left) and the phases of DTC migration (right). Ventral and dorsal body wall muscles are shown in blue. Gonad arms (yellow) are surrounded by basement membranes (green). The uncolored part corresponds to the lateral hypodermis. Two DTCs (red) are generated at the anterior and posterior ends of the gonad primordium, located at the ventral mid-body, and migrate in a U-shaped pattern during gonad development. DTC migration comprises three phases: the initial migration on the ventral body wall muscle (phase 1), the ventral-to-dorsal migration along the lateral hypodermis (phase 2) and the migration along the dorsal body wall muscle (phase 3) (Hedgecock et al., 1987; Su et al., 2000). (**B**-**G**) Nomarski images of the posterior gonad arms of wild-type (B), *mig-17(k174)* (C), *cogc-3(k181)* (D,E) and *cogc-1(k179)* hermaphrodites (F,G). The gonads exhibit a meandering morphology in *cogc-3(k181)* and *cogc-1(k179)* mutants. The migration paths of DTCs are depicted by orange lines and arrowheads. Anterior is leftwards. Dorsal is towards the top. A, anterior; P, posterior; D, dorsal; V, ventral. Scale bar: 25 μm. (**H**) Percentages of anterior (left) and posterior (right) gonad arms that underwent normal or defective DTC migration. The migration defects were scored as the earliest phase during which a defect was evident. *n*=120 for each experiment. (**I**) Genetic interactions of *mig-17* with *cogc-3* or *cogc-1*. Percentages of anterior and posterior gonad arms having phase 2 migration defects. *n*=120 for each experiment. The error bars represent the mean±s.d. The values were calculated from the data collected from the first and second half of the animals examined.

study the mechanism of MIG-17-dependent regulation of DTC migration, we analyzed two mutants, *cogc-3(k181)* and *cogc-1(k179)*, which were isolated spontaneously from the mutator strain *mut-7(pk204)*. These mutants have *mig-17*-like meandering DTC phenotypes (Fig. 1D-G). As in *mig-17* mutants, gonadal morphology in *cogc-3(k181)* and *cogc-1(k179)* mutants was highly variable, owing to the abnormal DTC migration. We classified the DTC migration phenotypes among *mig-17(k174), cogc-3(k181)* and *cogc-1(k179)* mutants with respect to the phase during which abnormal migration first became apparent (Fig. 1A). All three mutants had essentially the same DTC phenotypes: migration was normal during phase 1, the initial migration on the ventral body wall muscle, but migration became abnormal during phases 2 and 3 when the MIG-17 localizes to the gonadal basement membrane (Nishiwaki et al., 2000). DTC migration defects in *cogc-3(k181)* and *cogc-1(k179)* mutants were more severe and penetrant than those in the putative null mutant, *mig-17(k174)* (Fig. 1H). Both *cogc-3(k181)* and *cogc-1(k179)* mutants exhibited a protruding vulva phenotype.

cogc-3 and *cogc-1* act with *mig-17* in a common pathway

The phenotypic similarity between *cogc-3*, *cogc-1* and *mig-17* mutants suggests that COGC-3, COGC-1 and MIG-17 function in a common pathway controlling DTC migration. To test this possibility, we examined the genetic interactions between these genes using putative null alleles. Both *cogc-3(k181)* and *cogc-1(k179)* appeared to be null alleles, as discussed in a later section. When *cogc-3(k181)* or *cogc-1(k179)* was combined with *mig-17(k174)*, the defective DTC migration phenotypes were not enhanced and were similar to those seen in the single mutants *cogc-3(k181)* or *cogc-1(k179)* (Fig. 1I). These results, together with the fact that the defects in *cogc-3(k181)* and *cogc-1(k179)* mutants are more severe compared with *mig-17(k174)*, support the idea that *mig-17* acts in a common pathway with *cogc-3* and *cogc-1*, and that *mig-17* function is totally compromised in *cogc-3* and *cogc-1* mutants.

cogc-3 and *cogc-1* encode components of the COG complex

cogc-3 and *cogc-1* genes were cloned by genetic mapping and injection rescue experiments, and were mapped between *lin-17* and *unc-11* in linkage group *I*. Genetic mapping using single nucleotide polymorphisms (SNPs) placed *cogc-3* in the region between genomic clones W03D8 and Y54E10BL. Similarly, *cogc-1* was localized between Y54E10A and W05F2. Sequence analysis of the *cogc-3(k181)* genome identified a *Tc4* transposon insertion in exon 5 of the predicted gene *Y71F9AM.4a*, and the analysis of the *cogc-1(k179)* genome identified a *Tc1* transposon insertion in exon 8 of the predicted gene *Y54E10A.2*, which constituted a single gene with part of *Y54E10A.1* as determined by cDNA analysis (see Fig. S1 in the supplementary material). Both mutant phenotypes were rescued by injecting PCR products for the corresponding genomic regions (Fig. 2A). A series of RNA interference (RNAi) analyses suggested that the products from the longest mRNAs were responsible for *cogc-3* and *cogc-1* defects (see Fig. S1 in the supplementary material). Sequence analysis of *cogc-3* and *cogc-1* cDNAs revealed that the encoded proteins are homologs of human COG-3/Sec34 and COG-1/ldlBp, respectively. These proteins correspond to two of the four lobe A subunits of the bi-lobed hetero-octameric COG complex required for intracellular vesicle trafficking and Golgi function (Fig. 2B,C; Fig. 3A,B) (Chatterton et al., 1999; VanRheenen et al., 1999; Suvorova et al., 2001; Ungar et al., 2002). *cogc-3* comprises 14 exons encoding a predicted protein of 794 amino acids. The N terminus contains a coiled-coil domain that potentially acts in protein-protein interactions, whereas the C terminus has an EEA1-like domain that was originally identified in the EEA-1 protein, which tethers vesicles to endosomes (Christforidis et al., 1999; Loh and Hong, 2002). *cogc-1* comprises 15 exons encoding a predicted protein of 787 amino acids, and it also has an N-terminal coiled-coil domain (Fig. 2A,D).

All the putative components of the COG complex are required for DTC migration

Seven of the eight putative components of the *C. elegans* COG complex, including those corresponding to COGC-3 and COGC-1, have been identified based on their homology with mammalian and yeast components (Podos et al., 1994; Chatterton et al., 1999; Whyte and Munro, 2001). By searching sequence databases, we identified the remaining component, COGC-7, which is also encoded by the *C. elegans* genome (Fig. 3B). To test the role of each COG subunit in gonadal DTC migration, soaking RNAi experiments were performed in wild-type hermaphrodites at the first larval stage. The RNAi knockdown of any of the four components of lobe A, including both *cogc-3* and *cogc-1,* resulted in meandering DTC phenotypes similar to those seen in *cogc-3(k181)* and *cogc-1(k179)* mutants (Fig. 1D-G and Fig. 3C-F). We also observed similar DTC migration defects in RNAi knockdowns of lobe B components. Interestingly, RNAi of lobe A components caused a much stronger effect than that of lobe B components (Fig. 3G), consistent with the observations in yeast that mutations in lobe A components result in more severe growth defects than those in lobe B (Whyte and Munro, 2001). These results suggest that all eight COG components participate in a common pathway that regulates DTC migration and that each component is functionally distinct during this process.

COGC-1 coimmunoprecipitates with COGC-3

We performed western blot analysis using antibodies against the N termini of COGC-3 and COGC-1. The COGC-3 antibody detected an 87 kDa protein in wild-type animals that was not seen in the *cogc-3(k181)* mutant. In addition, the level of COGC-3 was lower in the *cogc-1(k179)* mutant (Fig. 4A). Likewise, the COGC-1 antibody detected an 83 kDa protein in wild-type animals that was not detected in the *cogc-1(k179)* mutant. As with the COGC-3 antibody data, the levels of COGC-1 were reduced in the *cogc-3(k181)* mutant (Fig. 4B). These results indicate that *cogc-3(k181)* and *cogc-1(k179)* are protein-null mutants and that COGC-3 and COGC-1 stabilize one another, although we cannot rule out the possibility that smaller isoforms of these proteins, undetectable by the antibodies, are still produced.

To examine whether COGC-3 and COGC-1 are incorporated in the same protein complex, we performed co-immunoprecipitation using wild-type worm lysate and anti-COGC-3. COGC-1 co-precipitated with COGC-3 in the presence of anti-COGC-3 but not with a control IgG (Fig. 4C,D), supporting the idea that COGC-3 and COGC-1 belong to the same protein complex.

COGC-3 expression

We performed immunohistochemistry to detect COGC-3 localization in situ. COGC-3 was detected in most tissues, including muscle, intestine and hypodermis. COGC-3 expression in the germline was very low, or nil. As observed in mammalian cells (Suvorova et al., 2001; Unger et al., 2002), COGC-3 staining was

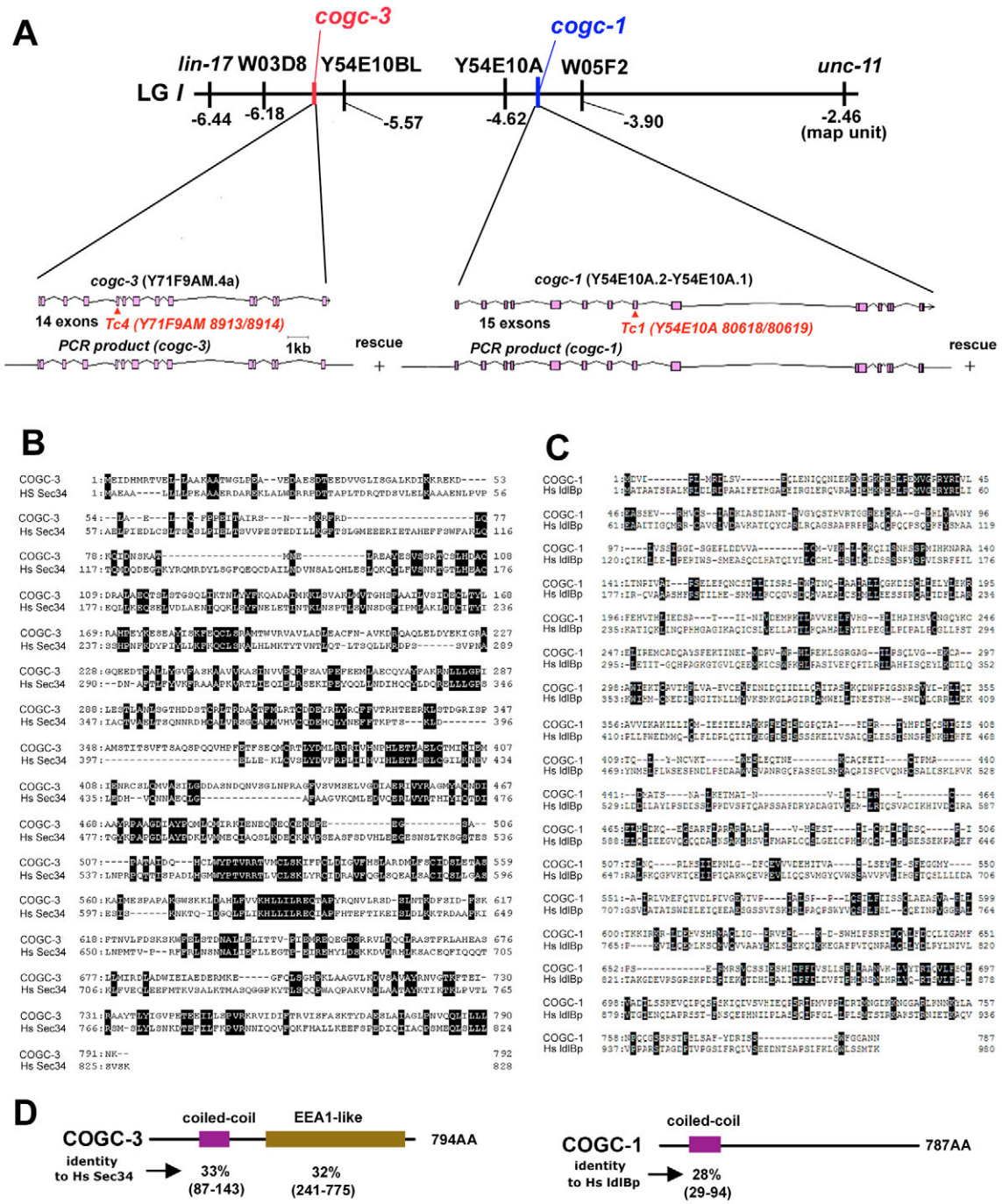

Fig. 2. Genetic mapping and molecular cloning of *cogc-3(k181)* and *cogc-1(k179)* mutants. (**A**) (Top) Genetic map of *cogc-3* and *cogc-1* loci. (Middle) The exon and intron structures of *cogc-3* and *cogc-1* genes. Arrowheads indicate the positions of transposon insertions. (Bottom) The PCR fragments used for injection rescue experiments. (**B**) Homology between COGC-3 and *Homo sapiens* (Hs) Sec34 (COG-3). (**C**) Homology between COGC-1 and Hs IdlBp (COG-1). Black boxes indicate identical amino acids. (**D**) Domain structures of COGC-3 and COGC-1. Conserved domains are shown in colored boxes with percentages of amino acid identity in human and *C. elegans* homologs. Amino acid positions in *C. elegans* proteins are shown in parentheses. The gene products of *cogc-3* and *cogc-1* correspond to the GenBank entries AB212858 and AB212859, respectively.

often prominent in the perinuclear region, which may correspond to the ER or Golgi apparatus (Fig. 5A-C). No signal was detected in *cogc-3(k181)* mutants (Fig. 5D), indicating that anti-COGC-3 specifically detected COGC-3 in situ. In whole-mount staining, COGC-3 was strongly expressed in cells of the pharynx, vulva and seam hypodermis (Fig. 5E-J), and of the intestine (data not shown). We examined the intracellular distribution of COGC-3 in the body wall muscle cells using a Golgi enzyme, MIG-23/NDPase (a type II membrane protein), as a marker. Some of the anti-COGC-3 signal colocalized with MIG-23-GFP, in particular, at the perinuclear region (Fig. 6A-C). We analyzed the colocalization of the COGC-3 and YFP-TRAM (Rolls et al., 2002), an ER-marker in the body wall muscle cells. COGC-3 was widely distributed in the cytoplasm and partially colocalized with YFP-TRAM (Fig. 6D-F).

MIG-23/NDPase is mislocalized in *cogc-3* and *cogc-1* mutants

It has been reported that Golgi type II membrane proteins are mislocalized or destabilized in culture cells harboring mutations in COG components (Bruinsma et al., 2004; Oka et al., 2004). Thus, we examined whether the pattern of MIG-23-GFP expression was affected in *cogc-3* and *cogc-1* mutants. Although the punctate cytoplasmic expression of MIG-23-GFP seen in wild-type worms was still observed, the intensity and number of the GFP signals were significantly reduced in *cogc-3* mutants (Fig. 6G,H). Furthermore, western blot analysis revealed that the amount of endogenous MIG-23 was also reduced in *cogc-3* and *cogc-1* mutants (Fig. 6O). The distribution of the ER marker mRFP-SP12 was not affected in *cogc-3* mutants (Fig. 6I-N). These results suggest that MIG-23 is destabilized in *cogc-3* and *cogc-1* mutants and that either the intracellular sorting of MIG-23 is severely altered or the structure of the MIG-23-associated Golgi apparatus is disorganized.

DTC migration requires COGC-3 expression in body wall muscle cells

MIG-17 is produced in and secreted from the body wall muscle cells (Nishiwaki et al., 2000). In the present study, we confirmed COGC-3 expression in these cells. If COGC-3 is required for MIG-17-mediated control of DTC migration, it is possible that this process requires COGC-3 expression in body wall muscle cells. The expression of *cogc-3*, which is controlled by the muscle-specific *unc-54* promoter, partially rescued the *cogc-3(k181)* phenotype; however, this phenotype was not rescued upon expression of *cogc-3* controlled by the touch neuron-specific *mec-7* promoter (Fig. 7A), suggesting that normal gonadal DTC migration requires COGC-3 activity in muscle cells, where MIG-17 is also expressed. One possible explanation of the partial rescue is that COGC-3 is also required in tissues besides muscle.

COGC-3 and COGC-1 are required for glycosylation and gonadal localization of MIG-17

cogc-3 and *cogc-1* encode components of the COG complex, which is required for intracellular vesicle trafficking and glycosylation. We therefore analyzed glycosylation and gonadal localization of MIG-17 in these mutant backgrounds. We compared the molecular sizes of MIG-17-GFP in wild type, *cogc-3(k181)* and *cogc-1(k179)* mutants using western blotting. The band at ~100 kDa, which corresponds to the MIG-17-GFP proform in wild-type worms, was broader and contained lower molecular weight species in the *cogc-3* and *cogc-1* mutants. The broadening was not due to the protein degradation in the mutants because treatment of the samples with PNGase F, which removes all *N*-glycans, yielded sharp bands of ~85 kDa both in wild type and mutants (Fig. 7B). These results indicate that MIG-17 glycosylation is incomplete in *cogc-3* and *cogc-1* mutants. We then examined the gonadal localization of MIG-17-GFP in both *cogc-3(k181)* and *cogc-1(k179)* mutants by immunostaining of worm cross-sections with anti-GFP. The MIG-17-GFP signal seen at the gonad surface in the wild type was almost undetectable in *cogc-3(k181)* and *cogc-1(k179)* mutants (Fig. 7C,D), indicating that the localization of MIG-17 is severely affected in these mutants.

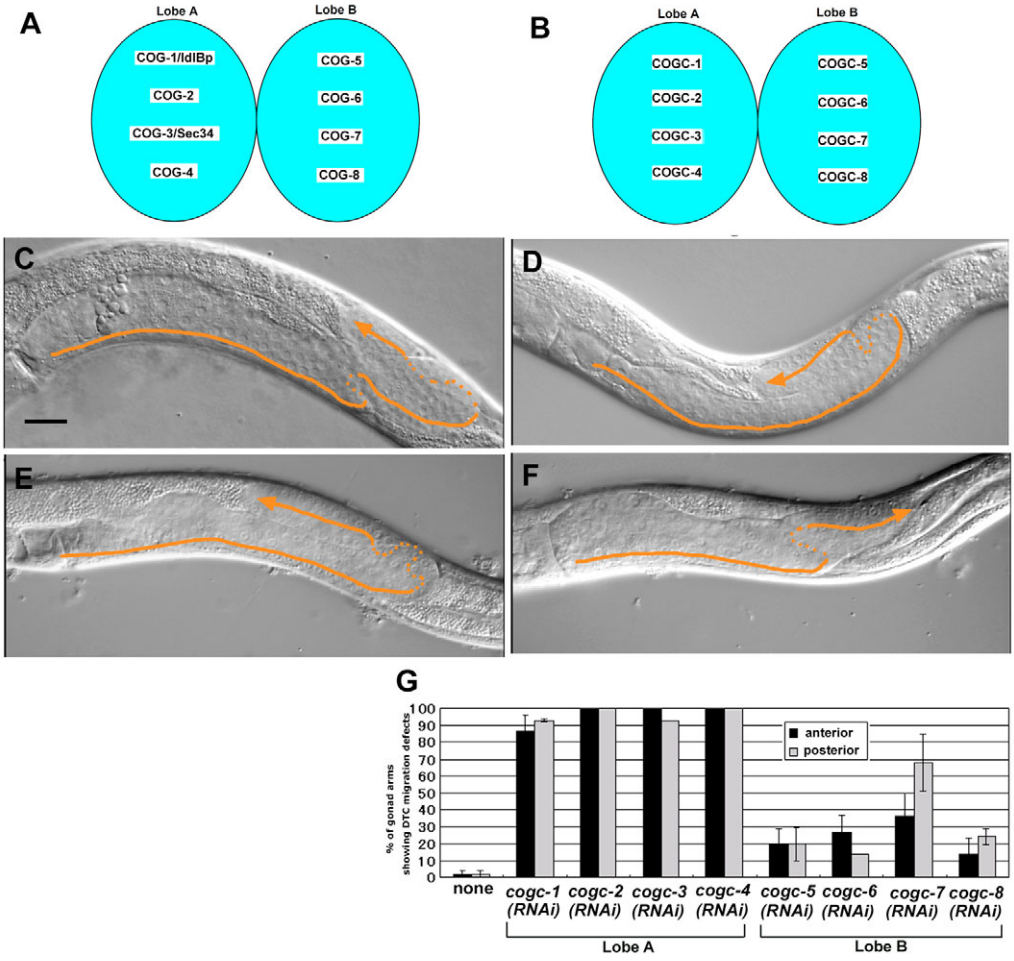

Fig. 3. RNA interference of components of the COG complex. Schematic diagrams of the COG complex in mammals (**A**) and *C. elegans* (**B**). Nomarski images of the posterior gonad arms of animals treated with RNAi directed against *cogc-1* (**C**), *cogc-2* (**D**), *cogc-3* (**E**) or *cogc-4* (**F**). Anterior is leftwards. Dorsal is towards the top. Scale bar: 25 μm. The migration paths of DTCs are depicted by orange lines and arrowheads. (**G**) Percentages of anterior and posterior gonad arms with DTC migration defects in RNAi knockdowns of COG components in the wild-type background. *n*=30 for each experiment. The following cDNAs were used for RNAi analysis of COG complex components: yk31b12 corresponds to *cogc-1*; yk324g6 to *C06G3.10/cogc-2*; yk863b10 to *cogc-3*; yk402e5 to *Y51H7C.6/cogc-4*; yk621c10 to *C43E11.1/cogc-5*; yk29e8 to *K07C11.9/cogc-6*; yk730h8 to *W01B6.9/cogc-7*; and yk26e9 to *R02D3.2/cogc-8*. The error bars represent the mean±s.d. The values were calculated from the data collected from the first and second half of the animals examined.

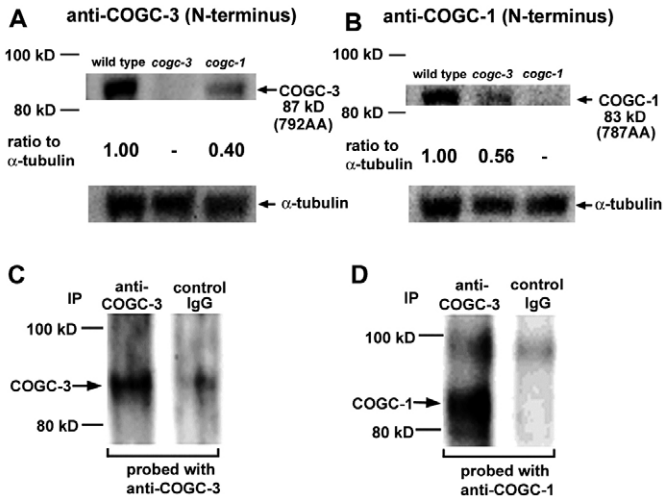

Fig. 4. COGC-3 and COGC-1 immunoblotting. Western blot analysis of COGC-3 (**A**) and COGC-1 (**B**). Protein lysates prepared from wild-type, *cogc-3* or *cogc-1* worms were immunoblotted with anti-COGC-3 or anti-COGC-1. α-tubulin was used as a loading control. (**C**,**D**) Co-immunoprecipitation experiments. Protein lysate prepared from wild-type worms was immunoprecipitated with anti-COGC-3 or normal rabbit IgG (negative control) and then immunoblotted with anti-COGC-3 (C) or anti-COGC-1 (D).

The localization defect of MIG-17 could be due either to the failure of secretion of MIG-17 from the muscle cells or to the loss of MIG-17 affinity for the gonadal basement membrane. To examine whether the secretory pathway functions normally in the muscle cells in *cogc-3* and *cogc-1* mutants, endocytotic uptake of GFP and MIG-17-Venus by coelomocytes was assessed according to the method of Fares and Greenwald (Fares and Greenwald, 2001a; Fares and Greenwald, 2001b). When we expressed either GFP containing the N-terminal secretion signal (ssGFP) or the MIG-17-Venus fusion protein in body wall muscle cells, both of these proteins localized to coelomocytes, which are scavenger cells that actively endocytose fluid from the pseudocoelom (Fig. 8A,D). Coelomocytes in *cogc-3* and *cogc-1* mutants showed normal accumulation of GFP and MIG-17-Venus (Fig. 8B,C,E,F). Moreover, MIG-17-Venus did not accumulate in the body wall muscle cells in these mutants (data not shown). These results indicate that MIG-17 is secreted normally from the muscle cells in *cogc-3* and *cogc-1* mutants.

MIG-17 is essential for COGC-3-mediated control of directed DTC migration

We asked whether the function of *cogc-3* in DTC migration is dependent on MIG-17. We addressed this problem by ectopically expressing MIG-17. MIG-17 is normally expressed in muscle cells, but ectopic expression in touch neurons under the control of the touch neuron-specific *mec-7* promoter also rescues DTC migration defects in *mig-17* mutants (Nishiwaki et al., 2004). Conceivably, MIG-17 secreted from touch neurons acts on the gonad to achieve normal DTC migration. However, MIG-17 expression in touch neurons of *cogc-3* mutants failed to rescue the DTC phenotypes. COGC-3 expression in touch neurons also failed to rescue *cogc-3*. By contrast, COGC-3 and MIG-17 co-expression in touch neurons substantially ameliorated the phase 2 DTC migration defects of *cogc-3* mutants (Fig. 9). The rescue of phase 3 defects was weak (data not shown). These results indicate that MIG-17 is functionally impaired in *cogc-3(k181)* mutants, implying that COGC-3 normally requires MIG-17 for its action in DTC migration. Thus, it is probable that COG components other than COGC-3 are also normally expressed in touch neurons.

DISCUSSION

Conservation of the COG complex across species

The COG complex is well conserved across species. All eight genes encoding the components of the COG complex, including COGC-3 and COGC-1, were identified in *C. elegans*. The *cogc-3(k181)*

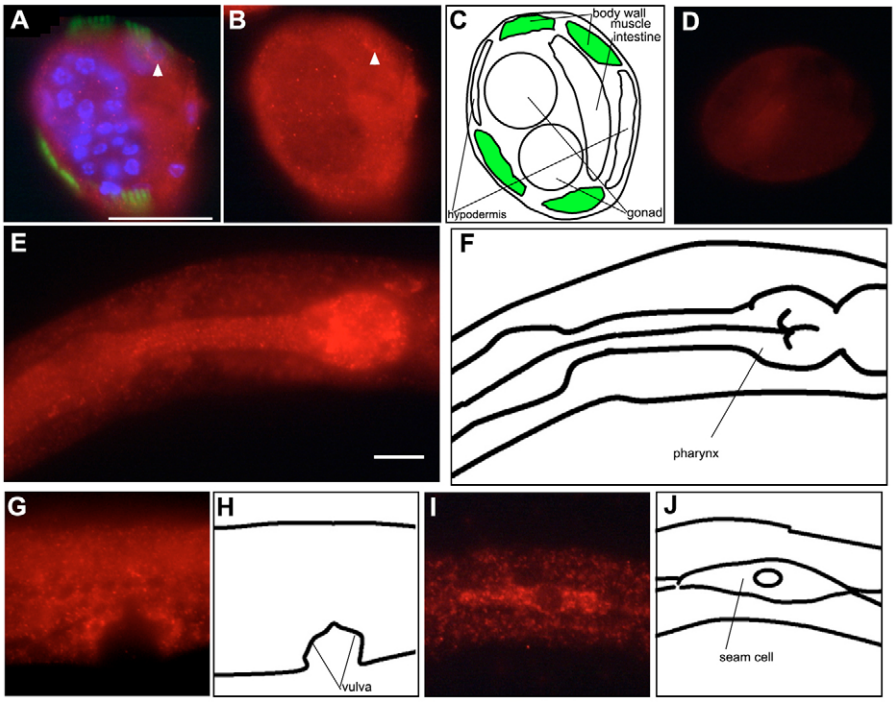

Fig. 5. Expression of COGC-3. (A-C) Immunolocalization of COGC-3 in a cross-section of a wild-type L4 larva. The section was stained with anti-COGC-3 (red), fluorescein phalloidin (green) and DAPI (blue). (**A**) Merged image. (**B**) Anti-COGC-3 image. (**C**) Schematic drawing of the positions of tissues. Arrowhead indicates the perinuclear localization of COGC-3 in a muscle cell. The muscle cells contain actin filaments stained by fluorescein phalloidin apically and the nuclei basally. (**D**) Localization of COGC-3 in a *cogc-3(k181)* L4 larva. No COGC-3 signal was detected. Dorsal is towards the top. Scale bar: 12.5 μm. (**E-J**) Whole-mount immunohistochemistry with COGC-3 antibody. Antibody staining patterns (EG,I) and corresponding schematic drawings (F,H,J) of wild-type L4 larvae. (E,F) Pharynx, (G,H) vulva and (I,J) seam cell. Dorsal is towards the top. Anterior is leftwards. Scale bar: 25 μm.

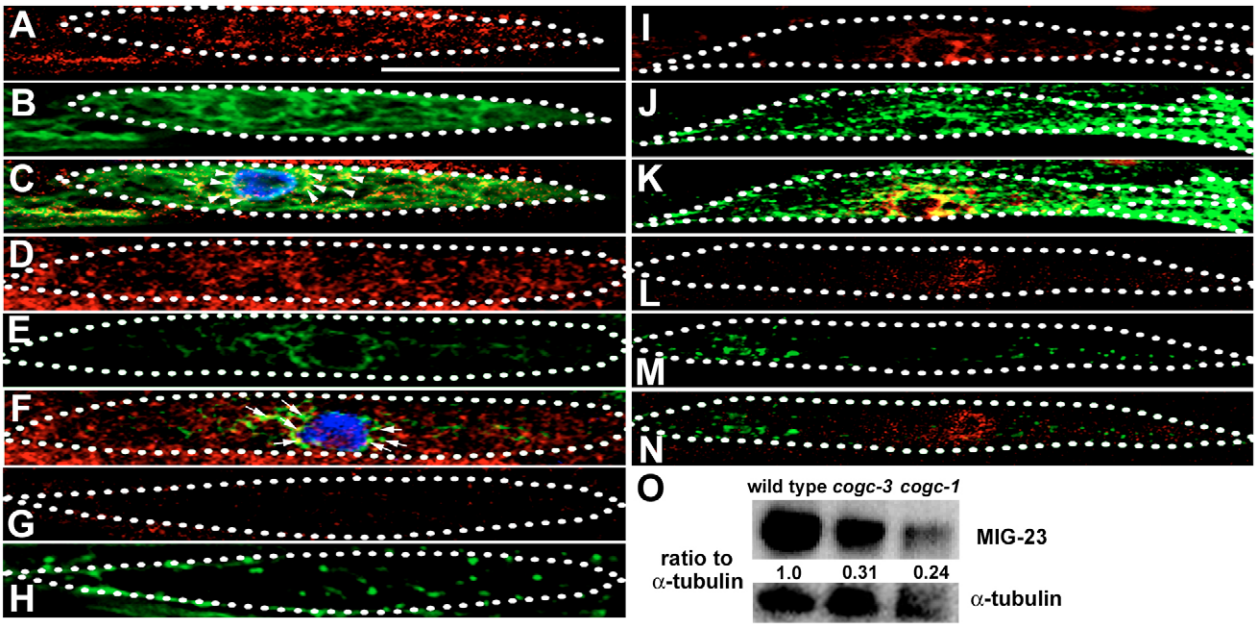

Fig. 6. Immunocytochemistry of COGC-3. (A-C) Confocal images of a body wall muscle cell of an L4 larva transgenic for *mig-23::GFP*. (**A**) Anti-COGC-3, (**B**) anti-GFP and (**C**) a merged image. Some of the COGC-3 signals colocalized with MIG-23-GFP (arrowheads). (D-F) Confocal images of a body wall muscle cell of an L4 larva transgenic for *YFP::TRAM*. (**D**) Anti-COGC-3, (**E**) anti-GFP and (**F**) a merged image. YFP-TRAM and COGC-3 signals colocalized at the perinuclear region (small arrows). (G,H) Confocal images of MIG-23-GFP in body wall muscle cells in *cogc-3(k181)* L4 larvae. (**G**) Anti-COGC-3 and (**H**) anti-GFP. The number and intensity of MIG-23-GFP signals were reduced. A similar result was obtained in *cogc-1(k179)* (data not shown). (**I-N**) Confocal images of mRFP-SP12 (I,L) and MIG-23-GFP (J,M) and merged images (K,N) in body wall muscle cells in wild-type (I-K) and *cogc-3(k181)* (L-N) L4 larvae. MIG-23-GFP partially colocalizes with mRFP-SP12 in wild type, but not in *cogc-3* mutants. The boundaries of the muscle cells are depicted by broken white lines. Scale bars: 25 μm. (**O**) Western blot of endogenous MIG-23. Protein lysates prepared from each strain were immunoblotted with anti-MIG-23 and anti-α-tubulin.

and *cogc-1(k179)* mutations in COG lobe A are probably null because the transposon insertions identified in these mutants are expected to produce termination codons. In fact, immunoblotting confirmed that these mutants are indeed null. However, worms carrying these mutations are viable and can proliferate as homozygotes, albeit very slowly. *cogc-1* RNAi in *cogc-3* mutants exacerbated the DTC migration defects (data not shown), suggesting that COGC-1 has other functions that are unrelated to COGC-3 function in gonadal DTC migration. These scenarios are very similar to those in the yeast lobe A mutants *cog1*, *cog2* or *cog3*, each of which grows very slowly and exhibit synthetic lethality when combined with each other (VanRheenen et al., 1999; Ram et al., 2002).

In mammalian cultured cells, the level of COG-1 is reduced when COG-3 is depleted (Zolov and Lupashin, 2005), but the level of COG-3 is not affected by depletion of COG-1 (Ungar et al., 2002; Oka et al., 2004). However, we observed in *C. elegans* that COGC-3 and COGC-1 stabilize each other. These results suggest that molecular interactions among the lobe A components in *C. elegans* may not be identical to those in mammals.

COG complex is required for stability of MIG-23/NDPase

COGC-3 is widely expressed in tissues such as the pharynx, vulva, seam hypodermis and body wall muscle. Using the maker protein MIG-23, a membrane-bound Golgi NDPase expressed in these muscle cells, we found that COGC-3 also localizes to the Golgi. Interestingly, colocalization of COGC-3 and MIG-23 was more clearly seen around nuclei than in the rest of the muscle cell cytoplasm. This could reflect differential distribution of these proteins in the Golgi compartments. The human Golgi NDPase is expressed widely in the Golgi (Wang and Guidotti, 1998), whereas the COG complex localizes primarily to the *cis*-Golgi, although it is also detected in other regions of the Golgi, including the late Golgi (Spelbrink et al., 1999; Kim et al., 2001; Suvorova et al., 2001). Thus, COG complex localization may follow a gradient that decreases from the early to late Golgi.

The punctate MIG-23-GFP expression was reduced in *cogc-3* and *cogc-1* mutants, suggesting that MIG-23 sorting or MIG-23-associated Golgi architecture may be perturbed in *cogc-3* and *cogc-1* mutants. When examined throughout larval development, this phenotype was not apparent during early stages and manifested during L4 and adult stages (see Fig. S2 in the supplementary material). As Golgi-resident enzymes such as NDPase are thought to be continuously sorted and recycled to the Golgi, the observation that this phenotype manifests only later in development might be due to abnormal development of Golgi structure. We also detected lower steady state levels of MIG-23-GFP in *cogc-3* and *cogc-1* mutants. A similar reduction in type II Golgi membrane proteins, such as mannosidase II, GOS-28, GS15, GPP130, CASP, giantin and golgin-84, have been reported in the ldlB and ldlC CHO cells (Oka et al., 2004).

COG complex is required for MIG-17 localization and glycosylation

MIG-17 was underglycosylated in *cogc-3* and *cogc-1* mutants. A number of studies have described functions for COG components in protein glycosylation. For example, glycosylation of invertase

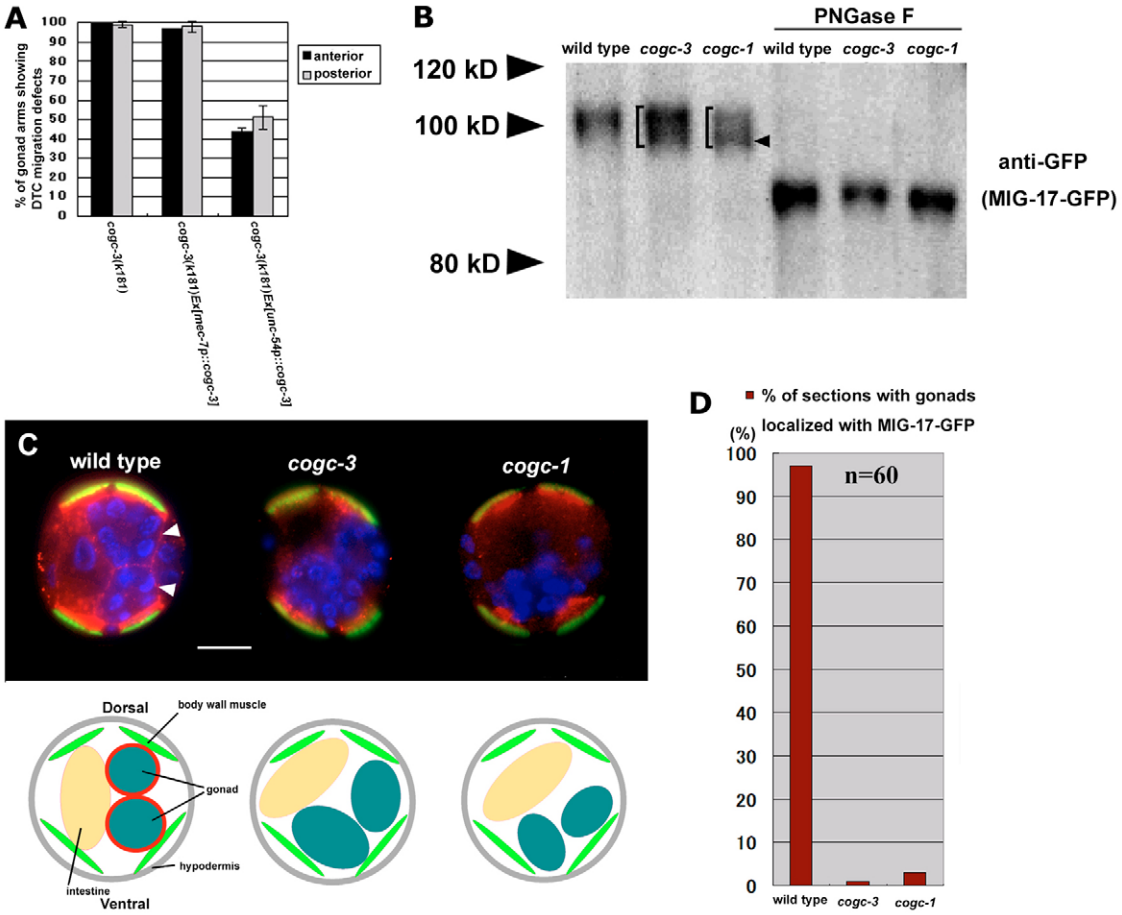

Fig. 7. MIG-17 glycosylation and localization in *cogc-3(k181)* and *cogc-1(k179)* mutants. (**A**) Percentages of anterior and posterior gonad arms with DTC migration defects in *cogc-3(k181)* worms carrying extrachromosomal transgenic arrays. *cogc-3* expression under the muscle-specific promoter *unc-54* rescues the DTC phenotype of *cogc-3* mutants. Both phase 2 and phase 3 defects were partially rescued (data not shown). The same transgenic array caused no DTC migration defects in wild-type background, indicating the partial rescue is not due to the overexpression of COGC-3. At least two independent lines were scored for transgenics, yielding similar results. Data for representative animals are shown. *n*=120 for each experiment. The error bars represent the mean±s.d. The values were calculated from the data collected from the first and second half of the animals examined. (**B**) *N*-glycosylation of MIG-17. Worm lysates were immunoprecipitated and immunoblotted with anti-GFP. The signals correspond to proforms of MIG-17-GFP. MIG-17-GFP in *cogc-3(k181)* and *cogc-1(k179)* mutants migrate further than wild-type MIG-17-GFP. Brackets indicate smearing of the bands in *cogc-3(k181)* and *cogc-1(k179)*. The underglycosylation of MIG-17-GFP is more prominent (arrowhead) in *cogc-1(k179)*. Part of each immunoprecipitate was treated with PNGase F (*N*-glycanase) and immunoblotted with anti-GFP. (**C**) Gonadal localization of MIG-17-GFP in cross sections (upper), and corresponding schematic diagrams (lower). Sections were stained with anti-GFP (red), fluorescein phalloidin (green) and DAPI (blue). The circular arrangement of nuclei in wild-type, *cogc-3(k181)* and *cogc-1(k179)* animals correspond to germ line nuclei of the gonads. Arrowheads indicate the gonadal localization of MIG-17-GFP to the surface of distal (upper) and proximal (lower) gonad arms in wild type. The gonadal localization is shown in red circles in the diagram. Dorsal is towards the top. Scale bar: 12.5 μm. (**D**) Quantitative analysis of MIG-17-GFP localization in wild type and mutants. *n*=60 for each experiment.

is defective in yeast mutants of *cog1*, *cog3*, *cog5*, *cog6*, *cog7* and *cog8* (Whyte and Munro, 2001), and the glycosylation and stability of the low-density lipoprotein receptor (LDLR) is affected in the CHO mutant cells ldlB and ldlC (Kingsley et al., 1986; Reddy and Krieger, 1989). In addition, multiple glycosylation pathways are disrupted in a type of human CDG caused by a mutation in COG-7 (Wu et al., 2004). Although we have previously reported that MIG-17 is underglycosylated and defective in gonadal localization in *mig-23* mutants (Nishiwaki et al., 2004), by comparison the defects in gonadal localization of MIG-17 in *cogc-3* and *cogc-1* mutants are more pronounced. These results raise the possibility that multiple glycosylation enzymes, including MIG-23/NDPase, are affected in *cogc-3* and *cogc-1* mutants.

We found that MIG-17 is secreted from the muscle cells of *cogc-3* and *cogc-1* mutants. As for protein secretion, the function of the COG complex appears to differ depending on the context. For example, in the yeast mutants *cog1* and *cog2*, secretion of many proteins is blocked (Kim et al., 2001), whereas secretion of invertase is delayed yet the extracellular secretion of the protein occurs at near wild-type levels (Bruinsma et al., 2004). Secretion of LDLR to the cell surface is not blocked in ldlB and ldlC cells (Kingsley et al., 1986; Reddy and Krieger, 1989). Thus, glycosylation and secretion of certain groups of proteins may be differentially dependent on the COG complex, implying separable functions for the complex. Alternatively, for many proteins, the COG complex may affect only the efficiency of secretion, and thus these proteins may be secreted slowly even in COG mutants.

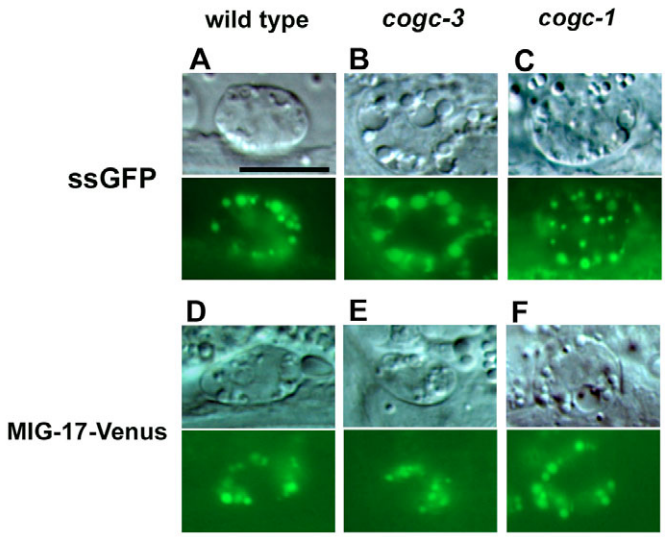

Fig. 8. Secretion of MIG-17-Venus. (**A-F**) Uptake of ssGFP (A-C) and MIG-17-Venus (D-F) secreted from muscles by wild type, *cogc-3* and *cogc-1* coelomocytes. Fluorescence images are shown beneath the Nomarski images of the same coelomocytes. All images were captured under the same exposure condition. Scale bar: 10 μm.

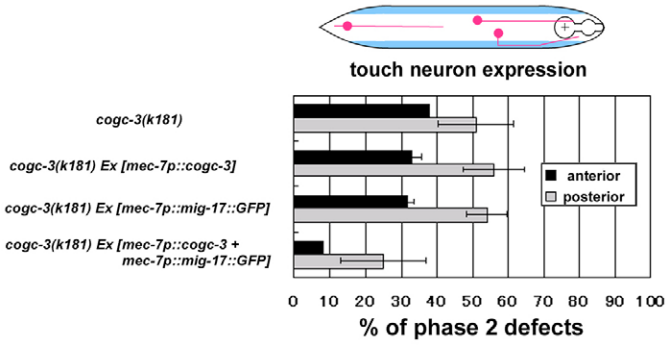

Fig. 9. Ectopic expression of MIG-17 and COGC-3 in touch neurons. (Top) Schematic diagram of touch neurons (red) on the right side of the worm. (Bottom) Percentages of anterior and posterior gonad arms with phase 2 DTC migration defects in *cogc-3(k181)* and strains expressing *cogc-3* and/or *mig-17::GFP* in touch neurons. More than two independent lines were scored for transgenics, yielding similar results. Data for representative animals are shown. *n*=120 for each experiment. The error bars represent the mean±s.d. The values were calculated from the data collected from the first and second half of the animals examined.

Function of the COG complex in gonad development

The ectopic co-expression of both COGC-3 and MIG-17, but not the individual proteins, in touch receptor neurons rescued the phase 2 migration defects of *cogc-3* mutants. Therefore, we conclude that COGC-3 regulates DTC migration through the action of MIG-17. Presumably, COGC-3 expressed in touch neurons facilitates the appropriate glycosylation of MIG-17, which is then secreted from the neurons and diffuses to the gonad where it controls DTC migration. Although we have not yet examined the functional link between the other COG components and MIG-17, the phenotypic similarity among the mutants and RNAi knockdowns suggests that all the COG components act together in MIG-17 glycosylation, which is essential for correct DTC migration. Although the defective phase 2 migration of *cogc-3* was strongly rescued by MIG-17 expression in touch neurons, the rescue of phase 3 defects was weak, suggesting that MIG-17 function is more important for phase 2 than for phase 3 migration. In addition, the defects in both phase 2 and 3 are more severe in *cogc-3* and *cogc-1* compared with *mig-17*. These results suggest that proteins other than MIG-17 are also affected by the COG complex. The protruding vulval phenotype observed in *cogc-3* and *cogc-1* mutants suggests this possibility. We performed lectin blot analysis using HRP-conjugated peanut agglutinin (PNA), a lectin with affinity for immature glycans (Wu et al., 2004). We found that PNA-binding activities were elevated in both *cogc-3* and *cogc-1* mutants (see Fig. S3 in the supplementary material), indicating that these mutations affect the glycosylation of multiple proteins.

In conclusion, we propose that the COG complex regulates the localization and stability of the Golgi enzymes involving MIG-23 and thereby affects the glycosylation and function of the MIG-17 ADAM protease, which is crucial for directed DTC migration. Our findings provide a model for the function of the COG complex in organ morphogenesis. Human CDG causes multisystemic abnormalities that include mental defects and malformation of organs (Marquardt and Denecke, 2003); however, although a mutation in COG-7 was found to affect the trafficking and function of the glycosylation machinery, the molecular mechanisms linking glycosylation defects to clinical presentations remain to be elucidated (Wu et al., 2004). Nonetheless, the functional genetic and molecular studies of the COG complex in *C. elegans* provide the molecular basis for understanding CDG and other glycosylation-dependent diseases.

We are grateful to Toshihiko Oka for suggestions for experiments, and to Toshihiko Oka, Kunihiro Matsumoto, Naoki Hisamoto and Shinji Ihara for critical reading of the manuscript. We thank Alan Couslon, Andy Fire, Yuji Kohara, Takeshi Ishihara, Hitoshi Sawa, Roger Y. Tsien, Hiroshi Kagoshima, Melissa M. Rolls, Tom A. Rapoport, Dmitry Poteryaev, Anne Spang, Theresa Stiernagle and the Caenorhabditis Genetics Center for materials; Asako Sugimoto for the soaking RNAi protocol. We also thank the members of our laboratory for discussions.

Supplementary material

Supplementary material for this article is available at
http://dev.biologists.org/cgi/content/full/133/2/263/DC1

References

Blelloch, R. and Kimble, J. (1999). Control of organ shape by a secreted metalloprotease in the nematode *C. elegans*. *Nature* **399**, 586-590.
Blelloch, R., Anna-Arriola, S. S., Gao, D., Li, Y., Hodgkin, J. and Kimble, J. (1999). The *gon-1* gene is required for gonadal morphogenesis in *C. elegans*. *Dev. Biol.* **216**, 382-393.
Brenner, S. (1974). The genetics of *Caenorhabditis elegans*. *Genetics* **77**, 71-94.
Bruinsma, P., Spelbrink, R. G. and Nothwehr, S. F. (2004). Retrograde transport of the mannosyltransferase Och1p to the early Golgi requires a component of the COG transport complex. *J. Biol. Chem.* **17**, 39814-39823.
Campbell, R. E., Tour, O., Palmer, A. E., Steinbach, P. A., Baird, G. S., Zacharias, D. A. and Tsien, R. Y. (2002). A monomeric red fluorescent protein. *Proc. Natl. Acad. Sci. USA* **99**, 7877-7882.
Chatterton, J. E., Hirsch, D., Schwartz, J. J., Bickel, P. E., Rosenberg, R. D., Lodish, H. F. and Krieger, M. (1999). Expression cloning of *LDLB*, a gene essential for normal Golgi function and assembly of the ldlCp complex. *Proc. Natl. Acad. Sci. USA* **96**, 915-920.
Christoforidis, S., McBride, H. M., Burgoyne, R. D. and Zerial, M. (1999). The Rab5 effector EEA1 is a core component of endosome docking. *Nature* **397**, 621-625.
Fares, H. and Greenwald, I. (2001a). Regulation of endocytosis by CUP-5, the *Caenorhabditis elegans* mucolipin-1 homolog. *Nat. Genet.* **28**, 64-68.
Fares, H. and Greenwald, I. (2001b). Genetic analysis of endocytosis in

Caenorhabditis elegans: coelomocyte uptake defective mutants. *Genetics* **159**, 133-145.
Farkas, R. M., Giansanti, M. G., Gatti, M. and Fuller, M. T. (2003). The *Drosophila Cog5* homologue is required for cytokinesis, cell elongation, and assembly of specialized Golgi architecture during spermatogenesis. *Mol. Biol. Cell* **14**, 190-200.
Hedgecock, E. M., Culotti, J. G., Hall, D. H. and Stern, B. D. (1987). Genetics of cell and axon migrations in *Caenorhabditis elegans*. *Development* **100**, 365-382.
Hedgecock, E. M., Culotti, J. G. and Hall, D. H. (1990). The *unc-5*, *unc-6*, and *unc-40* genes guide circumferential migrations of pioneer axons and mesodermal cells on the epidermis in *C. elegans*. *Neuron* **2**, 61-85.
Ishii, N., Wadsworth, W. G., Stern, B. D., Culotti, J. G. and Hedgecock, E. M. (1992). UNC-6, a laminin-related protein, guides cell and pioneer axon migrations in *C. elegans*. *Neuron* **9**, 873-881.
Kim, D.-W., Massey, T., Sacher, M., Pypaert, M. and Ferro-Novick, S. (2001). Sgf1p, a new component of the Sec34p/Sec35p complex. *Traffic* **2**, 820-830.
Kimble, J. and Hirsh, D. (1979). The postembryonic cell lineages of the hermaphrodite and male gonads in *Caenorhabditis elegans*. *Dev. Biol.* **70**, 396-417.
Kingsley, D. M., Kozarsky, K. F., Segal, M. and Krieger, M. (1986). Three types of low density lipoprotein receptor-deficient mutant have pleiotropic defects in the synthesis of N-liked, O-linked, and lipid-linked carbohydrate chains. *J. Cell Biol.* **102**, 1576-1585.
Krieger, M. M., Brown, S. and Goldstein, J. L. (1981). Isolation of Chinese hamster cell mutants with defects in the receptor-mediated endocytosis of low density lipoprotein. *J. Mol. Biol.* **150**, 167-184.
Loh, E. and Hong, W. (2002). Sec34 is implicated in traffic from the endoplasmic reticulum to the Golgi and exists in a complex with GTC-90 and ldlBp. *J. Biol. Chem.* **277**, 21955-21961.
Loh, E. and Hong, W. (2004). The binary interacting network of the conserved oligomeric Golgi tethering complex. *J. Biol. Chem.* **279**, 24640-24648.
Maduro, M. and Pilgrim, D. (1995). Identification and cloning of *unc-119*, a gene expressed in the *Caenorhabditis elegans* nervous system. *Genetics* **141**, 977-988.
Maeda, I., Kohara, Y., Yamamoto, M. and Sugimoto, A. (2001). Large-scale analysis of gene function in *Caenorhabditis elegans* by high-throughput RNAi. *Curr. Biol.* **11**, 171-176.
Marquardt, T. and Denecke, J. (2003). Congenital disorders of glycosylation: review of their molecular bases, clinical presentations and specific therapies. *Eur. J. Pediatr.* **162**, 359-379.
Mello, C. C., Kramer, J. M., Stichcomb, D. and Ambros, V. (1991). Efficient gene transfer in *C. elegans*: extrachromosomal maintenance and integration of transforming sequences. *EMBO J.* **10**, 3959-3970.
Nagai, T., Ibata, K., Park, E. S., Kubota, M., Mikoshiba, K. and Miyawaki, A. (2002). A variant of yellow fluorescent protein with fast and efficient maturation for cell-biological applications. *Nat. Biotechnol.* **20**, 87-90.
Nishiwaki, K. (1999). Mutations affecting symmetrical migration of distal tip cells in *Caenorhabditis elegans*. *Genetics* **152**, 985-997.
Nishiwaki, K., Hisamoto, N. and Matsumoto, K. (2000). A metalloprotease disintegrin that controls cell migration in *Caenorhabditis elegans*. *Science* **288**, 2205-2208.
Nishiwaki, K., Kubota, Y., Chigira, Y., Roy, S. M., Suzuki, M., Schvarzstein, M., Jigami, Y., Hisamoto, N. and Matsumoto, K. (2004). An NDPase links ADAM protease glycosylation with organ morphogenesis in *C. elegans*. *Nat. Cell Biol.* **6**, 31-37.
Nonet, M. L., Holgado, A. M., Brewer, F., Serpe, C. J., Norbeck, B. A., Holleran, J., Wei, L., Hartwieg, E., Jorgensen, E. M. and Alfonso, A. (1999). UNC-11, a *Caenorhabditis elegans* AP180 homologue, regulates the size and protein composition of synaptic vesicles. *Mol. Biol. Cell* **10**, 2343-2360.
Oka, T., Ungar, D., Hughson, F. M. and Krieger, M. (2004). The COG and COPI complexes interact to control the abundance of GEARs, a subset of Golgi integral membrane proteins. *Mol. Biol. Cell* **15**, 2423-2435.
Podos, S. D., Reddy, P., Ashkenas, J. and Krieger, M. (1994). *LDLC* encodes a brefeldin A-sensitive, peripheral Golgi protein required for normal Golgi function. *J. Cell Biol.* **127**, 679-691.
Poteryaev, D., Squirrell, J. M., Campbell, J. M., White, J. G. and Spang, A. (2005). Involvement of the actin cytoskeleton and homotypic membrane fusion in ER dynamics in *Caenorhabditis elegans*. *Mol. Biol. Cell* **16**, 2139-2153.
Ram, R. J., Li, B. and Kaiser, C. A. (2002). Identification of Sec36p, Sec37p, and Sec38p: components of yeast complex that contains Sec34p and Sec35p. *Mol. Biol. Cell* **13**, 1484-1500.
Reddy, P. and Krieger, M. (1989). Isolation and characterization of an extragenic suppressor of the low-density lipoprotein receptor-deficient phenotype of a Chinese hamster ovary cell mutant. *Mol. Cell. Biol.* **9**, 4799-4806.
Rolls, M. M., Hall, D. H., Victor, M., Stelzer, E. H. K., Rapoport, T. M. (2002). Targeting of rough endoplasmic reticulum membrane proteins and ribosomes in invertebrate neurons. *Mol. Biol. Cell* **13**, 1778-1791.
Sawa, H., Lobel, L. and Horvitz, H. R. (1996). The *Caenorhabditis elegans* gene *lin-17*, which is required for certain asymmetric cell divisions, encodes a putative seven-transmembrane protein similar to *Drosophila* Frizzled protein. *Genes Dev.* **10**, 2189-2197.
Serafini, T., Colamarino, S. A., Leonardo, E. D., Wang, H., Beddington, R., Skarmes, W. C. and Tessier-Lavigne, M. (1996). Netrin-1 is required for commissural axon guidance in the developing vertebrate nervous system. *Cell* **87**, 1001-1014.
Spelbrink, R. G. and Nothwehr, S. F. (1999). The yeast *GRD20* genes is required for protein sorting in the *trans*-Golgi network/endosomal system and polarization of the actin cytoskeleton. *Mol. Biol. Cell* **10**, 4263-4281.
Suvorova, E. S., Kurten, R. C. and Lupashin, V. V. (2001). Identification of a human orthologue of Sec34p as a component of the *cis*-Golgi vesicle tethering machinery. *J. Biol. Chem.* **276**, 22810-22818.
Suvorova, E. S., Duden, R. and Lupashin, V. V. (2002). The Sec34/Sec35p complex, a Ypt1p effector required for retrograde intra-Golgi trafficking, interacts with Golgi SNAREs and COPI vesicle coat proteins. *J. Cell Biol.* **157**, 631-643.
Ungar, D., Oka, T., Brittle, E. E., Vasile, E., Lupashin, V. V., Chatterton, J. E., Heuser, J. E., Krieger, M. and Waters, M. G. (2002). Characterization of a mammalian Golgi-localized protein complex, COG, that is required for normal Golgi morphology and function. *J. Cell Biol.* **157**, 405-414.
VanRheenen, S. M., Cao, X., Sapprerstein, S. K., Chiang, E. C., Lupashin, V. V., Barlowe, C. and Waters, M. G. (1999). Sec34p, a protein required for vesicle tethering to the yeast Golgi apparatus, is in a complex with Sec35p. *J. Cell Biol.* **147**, 729-742.
Wadsworth, W. G., Bhatt, H. and Hedgecock, E. M. (1996). Neuroglia and pioneer neurons express UNC-6 to provide global and local netrin cues for guiding migrations in *C. elegans*. *Neuron* **16**, 35-46.
Walter, D. M., Paul, K. S. and Waters, M. G. (1998). Purification and characterization of novel 13S hetero-oligomeric protein complex that stimulates *in vitro* Golgi transport. *J. Biol. Chem.* **273**, 29565-29576.
Wang, T.-F. and Guidotti, G. (1998). Golgi localization and functional expression of human uridine diphosphatase. *J. Biol. Chem.* **273**, 11392-11399.
Whyte, J. R. C. and Munro, S. (2001). The Sec34/35 Golgi transport complex is related to the exocyst, defining a family of complexes involved in multiple steps of membrane traffic. *Dev. Cell* **1**, 527-537.
Wicks, S. R., Yeh, R. T., Gish, W. R., Waterston, R. H. and Plasterk, R. H. (2001). Rapid gene mapping in *Caenorhabditis elegans* using a high density polymorphism map. *Nat. Genet.* **28**, 160-164.
Wu, X., Steet, R. A., Bohorov, O., Bakker, J., Newell, J., Krieger, M., Spaapen, L., Kornfeld, S. and Freeze, H. H. (2004). Mutation of the COG complex subunit gene *COG7* causes a lethal congenital disorder. *Nat. Med.* **10**, 518-523.
Wuestehube, L. J., Duden, R., Eun, A., Hamamoto, S., Korn, P., Ram, R. and Schekman, R. (1996). New mutants of *Saccharomyces cerevisiae* affected in the transport of proteins from endoplasmic reticulum to the Golgi complex. *Genetics* **142**, 393-406.
Yamaguchi, Y., Murakami, K., Furusawa, M. and Miwa, J. (1983). Germline-specific antigens identified by monoclonal antibodies in the nematode *C. elegans*. *Dev. Growth Differ.* **25**, 121-131.
Zolov, S. N. and Lupashin, V. V. (2005). Cog3p depletion blocks vesicle-mediated Golgi retrograde trafficking in HeLa cells. *J. Cell Biol.* **168**, 747-759.